Chapter 4

Low-energy QCD phenomenology

4.1 Quark potential models

Among the earliest approaches to QCD have been **quark potential models** describing quarks that move nonrelativistically within a hadron. The assumption is that the QCD interactions dress each quark with a cloud of virtual gluons and $q\bar{q}$ pairs and in this way transform it into a **constituent quark**, whose dynamical 'constituent mass' is so large that it becomes nonrelativistic. The energy levels and wave functions of hadrons are then obtained by solving a nonrelativistic Schrödinger equation using some assumed potential. While this strategy seems acceptable for truly massive quarks like b quarks, it becomes questionable for light u, d and s quarks where relativity and chiral symmetry complicate the dynamics (in fact, in Sec. 4.2 we will see how the dynamical breaking of chiral symmetry motivates the emergence of such constituent masses). Nevertheless, nonrelativistic quark models provide a framework for describing both ground and excited hadronic states and they have proven very useful for a basic understanding of their properties, in particular also for distinguishing 'ordinary' versus 'exotic' hadrons. In addition, with experimental indications for multiquark states, quark models have seen a revival in recent years.

The basic idea is to write down a Hamiltonian for a system of n quarks and/or antiquarks, where the interquark potential is typically the sum of two-body interactions:

$$H = \sum_{i=1}^{n} \frac{\boldsymbol{p}_i^2}{2m_i} + \sum_{i<j} V(\boldsymbol{r}_{ij})\,, \qquad \boldsymbol{r}_{ij} = \boldsymbol{r}_i - \boldsymbol{r}_j\,. \tag{4.1.1}$$

The Schrödinger equation

$$H\,\Psi_\lambda = E_\lambda \Psi_\lambda \tag{4.1.2}$$

then determines the binding energy E_λ and wave function Ψ_λ of a hadronic state $|\lambda\rangle$, whose mass is given by $M_\lambda = \sum_i m_i + E_\lambda$. Although there is no unique specification for the interquark potential V, it typically contains a spin- and flavor-dependent short-range potential, a spin- and flavor-independent long-range confining potential, basis mixing in the meson and baryon sectors, and relativistic corrections.

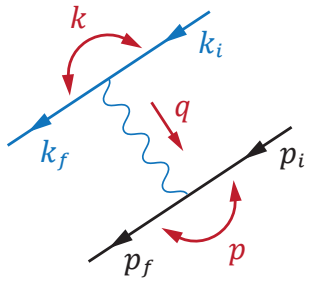

FIG. 4.1: One-photon exchange diagram between two fermions.

Breit-Fermi interaction. A useful starting point for constructing the potential $V(\boldsymbol{r}_{ij})$ is the nonrelativistic expansion of the **one-gluon exchange** interaction in a $q\bar{q}$ or qq system. The template for this is the analogous one-photon exchange amplitude in QED, e.g. between the electron and the proton in a hydrogen atom (Fig. 4.1), which is identical apart from the coupling, the masses and color factors:

$$\mathcal{M}_{\sigma\sigma'\lambda\lambda'}(q,p,k) = \frac{e^2}{q^2}\,\bar{u}_{\sigma'}(p_f)\,\gamma^\mu\,u_\sigma(p_i)\,\bar{u}_{\lambda'}(k_f)\,\gamma_\mu\,u_\lambda(k_i)\,. \tag{4.1.3}$$

We define three independent momenta q, p and k by

$$\begin{aligned} p_i &= p - \tfrac{q}{2}\,, & k_i &= k + \tfrac{q}{2}\,, \\ p_f &= p + \tfrac{q}{2}\,, & k_f &= k - \tfrac{q}{2}\,, \end{aligned} \qquad \Leftrightarrow \qquad q = p_f - p_i = k_i - k_f\,. \tag{4.1.4}$$

In the standard representation, the onshell spinors have the form

$$u_\sigma(p) = \sqrt{\frac{E_p + m}{2E_p}}\begin{bmatrix} \xi_\sigma \\ \boldsymbol{\alpha}\cdot\boldsymbol{\tau}\,\xi_\sigma \end{bmatrix}, \quad \boldsymbol{\alpha} = \frac{\boldsymbol{p}}{E_p + m}\,, \quad E_p = \sqrt{\boldsymbol{p}^2 + m^2}\,, \tag{4.1.5}$$

where m is the mass of the respective particle. The Pauli spinors satisfy $\xi^\dagger_{\sigma'}\xi_\sigma = \delta_{\sigma'\sigma}$, but note that we included a factor $1/\sqrt{2E_p}$ which corresponds to the 'nonrelativistic' Dirac spinor normalization $u^\dagger_{\sigma'}(p)\,u_\sigma(p) = \delta_{\sigma'\sigma}$.

To work out the non-relativistic expansion of the amplitude (4.1.3), we expand it in the three-momenta $\boldsymbol{q}$, $\boldsymbol{p}$ and $\boldsymbol{k}$. The spinors become

$$u_\sigma(p) \approx \begin{bmatrix} \left(1 - \frac{\boldsymbol{p}^2}{8m^2}\right)\xi_\sigma \\ \frac{\boldsymbol{p}\cdot\boldsymbol{\tau}}{2m}\,\xi_\sigma \end{bmatrix}, \qquad \bar{u}_\sigma(p) = u^\dagger_\sigma(p)\,\gamma^0 \approx \left[\xi^\dagger_\sigma\left(1 - \frac{\boldsymbol{p}^2}{8m^2}\right), -\xi^\dagger_\sigma\,\frac{\boldsymbol{p}\cdot\boldsymbol{\tau}}{2m}\right] \tag{4.1.6}$$

and the expansion of the factor $1/q^2$ in front of the amplitude yields

$$q^2 \approx -\boldsymbol{q}^2 + \frac{(\boldsymbol{p}\cdot\boldsymbol{q})(\boldsymbol{q}\cdot\boldsymbol{k})}{m_1 m_2} \quad \Rightarrow \quad \frac{1}{q^2} \approx -\frac{1}{\boldsymbol{q}^2}\left(1 + \frac{(\boldsymbol{p}\cdot\hat{\boldsymbol{q}})(\hat{\boldsymbol{q}}\cdot\boldsymbol{k})}{m_1 m_2}\right), \tag{4.1.7}$$

where $\hat{\boldsymbol{q}} = \boldsymbol{q}/|\boldsymbol{q}|$. Employing the γ-matrices in the standard representation, the resulting amplitude is

$$\begin{aligned} \mathcal{M}(\boldsymbol{q},\boldsymbol{p},\boldsymbol{k}) \approx -\frac{4\pi\alpha}{\boldsymbol{q}^2}\Bigg[1 - \frac{\boldsymbol{q}^2}{8}\left(\frac{1}{m_1^2} + \frac{1}{m_2^2}\right) - \frac{\boldsymbol{p}\cdot\boldsymbol{k} - (\boldsymbol{p}\cdot\hat{\boldsymbol{q}})(\boldsymbol{k}\cdot\hat{\boldsymbol{q}})}{m_1 m_2} - \frac{(\boldsymbol{q}\times\boldsymbol{s}_1)\cdot(\boldsymbol{q}\times\boldsymbol{s}_2)}{m_1 m_2} \\ + \frac{i\boldsymbol{s}_1\cdot(\boldsymbol{q}\times\boldsymbol{p})}{2m_1^2} - \frac{i\boldsymbol{s}_2\cdot(\boldsymbol{q}\times\boldsymbol{k})}{2m_2^2} - \frac{i\boldsymbol{s}_1\cdot(\boldsymbol{q}\times\boldsymbol{k}) - i\boldsymbol{s}_2\cdot(\boldsymbol{q}\times\boldsymbol{p})}{m_1 m_2}\Bigg] \end{aligned} \tag{4.1.8}$$

with $\alpha = e^2/(4\pi)$. Here we suppressed the polarization indices by dropping the unit matrices $\delta_{\sigma'\sigma}\,\delta_{\lambda'\lambda}$ in the notation and introducing the spin vectors

$$(\boldsymbol{s}_1)_{\sigma'\sigma} = \chi^\dagger_{\sigma'}\,\frac{\boldsymbol{\tau}}{2}\,\chi_\sigma\,, \qquad (\boldsymbol{s}_2)_{\lambda'\lambda} = \chi^\dagger_{\lambda'}\,\frac{\boldsymbol{\tau}}{2}\,\chi_\lambda\,. \tag{4.1.9}$$

Note that all instances of $\boldsymbol{p}$ and $\boldsymbol{k}$ in the above expression are transverse in $\boldsymbol{q}$, so we could as well replace $\boldsymbol{p} \to \boldsymbol{p}_{i,f}$ and $\boldsymbol{k} \to \boldsymbol{k}_{i,f}$ which only differ by $\pm\boldsymbol{q}/2$. Finally, we take the Fourier transform with respect to $\boldsymbol{q}$ using

$$\int\frac{d^3q}{(2\pi)^3}\,\frac{e^{i\boldsymbol{q}\cdot\boldsymbol{r}}}{\boldsymbol{q}^2}\begin{bmatrix}1\\ \boldsymbol{q}\\ \boldsymbol{q}^2\\ q_i\,q_j\\ \dfrac{q_i\,q_j}{\boldsymbol{q}^2}\end{bmatrix} = \frac{1}{4\pi r}\begin{bmatrix}1\\ \dfrac{i\boldsymbol{r}}{r^2}\\ 4\pi r\,\delta^3(\boldsymbol{r})\\ \dfrac{1}{r^2}\,(\delta_{ij}-3\,\hat r_i\,\hat r_j)+\dfrac{4\pi r}{3}\,\delta^3(\boldsymbol{r})\,\delta_{ij}\\ \frac{1}{2}\,(\delta_{ij}-\hat r_i\,\hat r_j)\end{bmatrix}, \tag{4.1.10}$$

where $\hat{\boldsymbol{r}} = \boldsymbol{r}/r$ and $r = |\boldsymbol{r}|$, to arrive at the final expression below.

The resulting **Breit-Fermi interaction** is the three-dimensional Fourier transform of the one-photon exchange amplitude (4.1.3) in the non-relativistic limit:

$$\begin{aligned} V(\boldsymbol{r},\boldsymbol{p},\boldsymbol{k}) &= \int\frac{d^3q}{(2\pi)^3}\,e^{i\boldsymbol{q}\cdot\boldsymbol{r}}\,\mathcal{M}(\boldsymbol{q},\boldsymbol{p},\boldsymbol{k}) \\ &= \alpha\left[-\frac{1}{r}+T_{\rm d}+\frac{T_{\rm o}}{r}+\frac{8\pi}{3}\,\delta^3(\boldsymbol{r})\,T_{\rm ss}+\frac{T_{\rm ten}+T^{(1)}_{\rm so}+T^{(2)}_{\rm so}}{r^3}\right]. \end{aligned} \tag{4.1.11}$$

It is identical for a fermion-fermion and fermion-antifermion system, and apart from the color factor (which we discuss below) it can be directly carried over to QCD to establish a non-relativistic qq and $q\bar q$ interaction potential between (onshell) quarks.

■ The first three terms in Eq. (4.1.11) are the Coulomb term, the Darwin term and the orbit-orbit interaction, which are all spin-independent:

$$T_{\rm d} = \frac{\pi}{2}\left(\frac{1}{m_1^2}+\frac{1}{m_2^2}\right)\delta^3(\boldsymbol{r}), \qquad T_{\rm o} = \frac{\boldsymbol{p}\cdot\boldsymbol{k}+(\boldsymbol{p}\cdot\hat{\boldsymbol{r}})(\boldsymbol{k}\cdot\hat{\boldsymbol{r}})}{2m_1m_2}\,. \tag{4.1.12}$$

■ The next two terms constitute the **hyperfine interaction**, which consists of a spin-spin contact term and a tensor force:

$$T_{\rm ss} = \frac{\boldsymbol{s}_1\cdot\boldsymbol{s}_2}{m_1m_2}\,, \qquad T_{\rm ten} = \frac{3\,(\boldsymbol{s}_1\cdot\hat{\boldsymbol{r}})\,(\boldsymbol{s}_2\cdot\hat{\boldsymbol{r}})-\boldsymbol{s}_1\cdot\boldsymbol{s}_2}{m_1m_2}\,. \tag{4.1.13}$$

It arises from a magnetic dipole-dipole interaction, since the Fourier transform of the term $(\boldsymbol{q}\times\boldsymbol{s}_1)\cdot(\boldsymbol{q}\times\boldsymbol{s}_2)$ is proportional to

$$(\boldsymbol{s}_1\times\boldsymbol{\nabla})\cdot(\boldsymbol{s}_2\times\boldsymbol{\nabla})\,\frac{1}{r} = \boldsymbol{s}_1\cdot\left[\boldsymbol{\nabla}\times\left((\boldsymbol{s}_2\times\boldsymbol{\nabla})\,\frac{1}{r}\right)\right] \propto \boldsymbol{s}_1\cdot\boldsymbol{B}_2\,, \tag{4.1.14}$$

where $\boldsymbol{B}_2$ is the magnetic field produced by the magnetic dipole moment $\boldsymbol{s}_2$. Spin-spin interactions of the form $\boldsymbol{s}_1\cdot\boldsymbol{s}_2$ in the Hamiltonian induce level splittings between states with different spin, which leads to mass formulas of the form

$$H = \cdots + c\,\boldsymbol{s}_1\cdot\boldsymbol{s}_2 + \ldots \quad\Rightarrow\quad M = \cdots + c\,\langle\boldsymbol{s}_1\cdot\boldsymbol{s}_2\rangle + \ldots \tag{4.1.15}$$

If we write the total spin of a two-fermion system as $\boldsymbol{S} = \boldsymbol{s}_1 + \boldsymbol{s}_2$, we have

$$\boldsymbol{S}^2 = \boldsymbol{s}_1^2 + \boldsymbol{s}_2^2 + 2\boldsymbol{s}_1 \cdot \boldsymbol{s}_2 \quad \Rightarrow \quad \langle \boldsymbol{s}_1 \cdot \boldsymbol{s}_2 \rangle = \frac{S(S+1) - \frac{3}{2}}{2}\,, \tag{4.1.16}$$

which generates the mass splittings between pseudoscalar ($S = 0$) and vector mesons ($S = 1$). For baryons, the hyperfine interaction is responsible for the dominant mass splittings between the ground-state octet ($S = \frac{1}{2}$) and decuplet baryons ($S = \frac{3}{2}$).

- The remaining two terms constitute the **spin-orbit interaction**:

$$T_{\rm so}^{(1)} = \frac{\boldsymbol{s}_1 \cdot (\boldsymbol{r} \times \boldsymbol{p})}{2m_1^2} - \frac{\boldsymbol{s}_2 \cdot (\boldsymbol{r} \times \boldsymbol{k})}{2m_2^2}\,, \qquad T_{\rm so}^{(2)} = \frac{\boldsymbol{s}_2 \cdot (\boldsymbol{r} \times \boldsymbol{p}) - \boldsymbol{s}_1 \cdot (\boldsymbol{r} \times \boldsymbol{k})}{m_1 m_2}\,. \tag{4.1.17}$$

For example, for $m_1 = m_2 = m$ and in the frame where $\boldsymbol{k} = -\boldsymbol{p}$, this yields

$$T_{\rm so}^{(1)} + T_{\rm so}^{(2)} = \frac{3\,(\boldsymbol{s}_1 + \boldsymbol{s}_2) \cdot \boldsymbol{L}}{2m^2} = \frac{3\,\boldsymbol{L} \cdot \boldsymbol{S}}{2m^2}\,, \qquad \boldsymbol{L} = \boldsymbol{r} \times \boldsymbol{p}\,. \tag{4.1.18}$$

The resulting mass splittings can be estimated from $\boldsymbol{J}^2 = (\boldsymbol{L} + \boldsymbol{S})^2$ as

$$\langle \boldsymbol{L} \cdot \boldsymbol{S} \rangle = \frac{1}{2}\,(J(J+1) - L(L+1) - S(S+1))\,. \tag{4.1.19}$$

For orbital ground states ($L = 0$ and thus $J = S$) the spin-orbit interaction does not contribute. For $L = S \neq 0$, it leads to splittings between states with different J, e.g. for the charmonium states $\{\chi_{c0}, \chi_{c1}, \chi_{c2}\}$ with $J^{PC} = \{0, 1, 2\}^{++}$, which carry $S = L = 1$ and only differ in their total angular momentum J (see Fig. 3.14):

$$\langle \boldsymbol{L} \cdot \boldsymbol{S} \rangle = \frac{1}{2}\,(J(J+1) - 4) = \{-2, -1, 2\}\,. \tag{4.1.20}$$

For baryons, spin-orbit interactions are generally small and usually neglected. (In the hydrogen atom with $m_e \ll m_p$, the spin-orbit force beats the spin-spin interaction and gives rise to the atomic **fine structure** effects.)

It turns out that Eq. (4.1.11) is quite general. If we had started from a different amplitude with scalar, pseudoscalar, axialvector or tensor particle exchanges, we could still split the resulting potential into spin-independent and spin-dependent terms:

$$V = V_0 + (\dots) + V_{\rm ss}\,T_{\rm ss} + V_{\rm ten}\,T_{\rm ten} + V_{\rm so}^{(1)}\,T_{\rm so}^{(1)} + V_{\rm so}^{(2)}\,T_{\rm so}^{(2)}\,. \tag{4.1.21}$$

The spin-dependent terms can be expressed through derivatives of $V_0(r)$, e.g., for a general vector-exchange potential one finds

$$V_{\rm ss} = \frac{2}{3}\,\Delta V_0\,, \qquad V_{\rm ten} = \frac{1}{3}\left(\frac{V_0'}{r} - V_0''\right), \qquad V_{\rm so}^{(1)} = V_{\rm so}^{(2)} = \frac{V_0'}{r}\,, \tag{4.1.22}$$

where Δ is the Laplace operator and a Coulomb potential corresponds to $V_0 = -1/r$. A scalar exchange only leads to a spin-orbit interaction,

$$V_{\rm so}^{(1)} = -\frac{V_0'}{r}\,, \qquad V_{\rm ss} = V_{\rm ten} = V_{\rm so}^{(2)} = 0\,, \tag{4.1.23}$$

whereas a pseudoscalar exchange does not produce spin-dependent terms at all. Axialvector and tensor exchanges only contribute to $V_{\rm ss}$.

Color factors. In order to apply the Breit-Fermi potential to QCD, where the photon is replaced by a gluon, we must also work out the color algebra since gluons couple to quarks through the $SU(3)_c$ generators t_a. If we denote the generators in an arbitrary $SU(3)$ representation by $\hat{\mathsf{t}}_a$ and write

$$\mathbf{t}^2 = \sum_a \hat{\mathsf{t}}_a^2 = C(R)\,, \tag{4.1.24}$$

then the Casimir in a general $SU(3)$ representation is given by

$$C(R) = \frac{3p + 3q + p^2 + pq + q^2}{3}\,, \tag{4.1.25}$$

where p and q are the quantum numbers that label the multiplets, cf. Eq. (B.2.7) in the appendix. This yields

$$C(\mathbf{1}) = 0\,, \quad C(\mathbf{3}) = C(\overline{\mathbf{3}}) = \frac{4}{3}\,, \quad C(\mathbf{6}) = C(\overline{\mathbf{6}}) = \frac{10}{3}\,, \quad C(\mathbf{8}) = 3\,, \quad \text{etc.} \tag{4.1.26}$$

If we write

$$\mathbf{t}_1 \cdot \mathbf{t}_2 = \sum_a \hat{\mathsf{t}}_a \otimes \hat{\mathsf{t}}_a\,, \tag{4.1.27}$$

where 1 and 2 refer to the particles on which they act, then the generator in the product space is $\mathbf{t}_{12} = \mathbf{t}_1 + \mathbf{t}_2$ with $\mathbf{t}_{12}^2 = C_{12}$, $\mathbf{t}_1^2 = C_1$ and $\mathbf{t}_2^2 = C_2$. As a consequence,

$$\mathbf{t}_{12}^2 = \mathbf{t}_1^2 + \mathbf{t}_2^2 + 2\,\mathbf{t}_1 \cdot \mathbf{t}_2 \quad \Rightarrow \quad \mathbf{t}_1 \cdot \mathbf{t}_2 = \frac{C_{12} - C_1 - C_2}{2}\,. \tag{4.1.28}$$

For an attractive color potential we must have $\mathbf{t}_1 \cdot \mathbf{t}_2 < 0$. Because quarks and antiquarks live in the $\mathbf{3}$ and $\overline{\mathbf{3}}$ representations, one has $C_1 = C_2 = \frac{4}{3}$ both for $q\bar{q}$ and qq systems which entails $C_{12} < \frac{8}{3}$ for an attractive potential. From Eq. (4.1.26) this only leaves color-singlet mesons and color-antitriplet diquarks (or color-triplet antidiquarks):

$$C_{12}(\mathbf{1}) = 0 \quad \Rightarrow \quad \mathbf{t}_1 \cdot \mathbf{t}_2 = -\frac{4}{3}\,, \qquad C_{12}(\overline{\mathbf{3}}) = \frac{4}{3} \quad \Rightarrow \quad \mathbf{t}_1 \cdot \mathbf{t}_2 = -\frac{2}{3}\,. \tag{4.1.29}$$

Thus, the $q\bar{q}$ color interaction in the color-singlet meson channel is maximally attractive, whereas in the color-octet channel with $C_{12}(\mathbf{8}) = 3$ it is repulsive. Likewise, the interaction between two quarks in the $\overline{\mathbf{3}}$ channel is attractive, with a color factor half as strong as for mesons, whereas in the $\mathbf{6}$ channel it is repulsive. This is relevant for the binding of baryons, since from

$$\mathbf{3} \otimes \mathbf{3} \otimes \mathbf{3} = (\overline{\mathbf{3}} \oplus \mathbf{6}) \otimes \mathbf{3} = \mathbf{1} \oplus \mathbf{8} \oplus \mathbf{8} \oplus \mathbf{10} \tag{4.1.30}$$

a $\overline{\mathbf{3}}$ diquark can bind together with the remaining quark to form a color-singlet baryon. One can furthermore show that

$$f_{abc}\,(\mathsf{t}_a)_{il}\,(\mathsf{t}_b)_{jm}\,(\mathsf{t}_c)_{kn}\,\varepsilon_{lmn} = 0\,. \tag{4.1.31}$$

This is the color factor stemming from a three-gluon vertex (f_{abc}) that is connected to three quarks, which are then contracted with the antisymmetric color wave function of a baryon (ε_{lmn}). Hence, the leading three-body force in a baryon mediated by a three-gluon vertex vanishes! This suggests that the internal structure of baryons is dominated by two-body forces in the attractive $\overline{\mathbf{3}}$ diquark channels.

Potential in QCD. What would the interquark potential look like in QCD?

- At short distances, by means of asymptotic freedom, we expect a **Coulomb**-like potential $V(r) \propto -1/r$ mediated by the massless gluon. Here we could take over the Breit-Fermi interaction (4.1.11), replace $\alpha \to \alpha_s$ and attach a color factor $4/3$ for the $q\bar{q}$ interaction and $2/3$ for the qq interaction (the minus signs are already implicit, e.g. in the Coulomb term), or just start with the Coulomb term alone.
- At large distances, we expect a linear **confinement** potential $V_{\text{conf}} = \sigma r$, where σ is called the string tension. This is motivated from several angles, including the observed mass orderings (Regge phenomenology) and lattice calculations of the Wilson loop in pure Yang-Mills theory.

Two examples of how to interpolate between a single gluon exchange at short distances and confinement at large distances are the **Cornell** and **Richardson** potentials:

$$\begin{aligned} V_C(r) &= -\frac{4\alpha_s}{3r} + \sigma r\,, \\ V_R(r) &= -\frac{4}{3}\frac{(4\pi)^2}{\beta_0}\,\text{FT}\left[\frac{1}{\boldsymbol{q}^2\,\ln(1+\boldsymbol{q}^2/\Lambda^2)}\right], \end{aligned} \tag{4.1.32}$$

where the latter also incorporates asymptotic freedom in terms of a logarithmic running of the coupling (FT denotes the Fourier transform).

From the discussion around Eq. (4.1.21), the generic structure of the potential is not limited to a gluon exchange. For example, we could distribute the confinement potential between a scalar and vector exchange potential by a parameter $0 \leq \xi \leq 1$,

$$V_0 = V_S + V_V = (1-\xi)\,\sigma r + \left(\xi\,\sigma r - \frac{a}{r}\right), \tag{4.1.33}$$

where $\xi = 0$ corresponds to scalar confinement and $\xi = 1$ to vector confinement. According to Eqs. (4.1.22–4.1.23), this yields

$$V = V_0 + (\dots) + \frac{2}{3}\Delta V_V\,T_{\text{ss}} + \frac{1}{3}\left(\frac{V_V'}{r} - V_V''\right)T_{\text{ten}} + \frac{V_V' - V_S'}{r}\,T_{\text{so}}^{(1)} + \frac{V_V'}{r}\,T_{\text{so}}^{(2)}\,. \tag{4.1.34}$$

Fits to the charmonium spectrum based on this expression have suggested that confinement is predominantly **scalar**.

One should keep in mind that the concept of a *potential* does not account for the full dynamics as it assumes interactions to be instantaneous. More generally, one expects a large-distance behavior $\propto r$ for the $q\bar{q}$ four-point function in Eq. (3.1.135), since this is the quantity related to the Wilson loop (for infinitely heavy static quarks). The dynamical origin of confinement is still under debate and has been attributed to **center vortices**, or to the formation of color-electric flux tubes and the condensation of color-magnetic monopoles in the **dual superconductor** picture. Diagrammatically, it is conceivable that confinement may only arise from complicated combinations of gluon exchanges. On the other hand, the full quark-gluon vertex in QCD has a more general structure than the γ^μ part, cf. Eq. (2.3.16), and a gluon exchange with a full propagator and full vertices also contains scalar parts. In Landau gauge, the scaling solution mentioned below Eq. (2.3.25) indeed generates a $q\bar{q}$ interaction $\propto 1/q^4$ which leads to a linear rise in coordinate space.

Quark models for baryons. In order to construct a Hamiltonian (4.1.36) for baryons with $n = 3$, let us assume equal constituent masses $m_i = m$. It is convenient to introduce a center-of-mass coordinate $\boldsymbol{R}$ and two relative coordinates $\boldsymbol{\rho}$ and $\boldsymbol{\lambda}$,

$$\boldsymbol{R} = \frac{\boldsymbol{r}_1 + \boldsymbol{r}_2 + \boldsymbol{r}_3}{\sqrt{3}}\,, \quad \boldsymbol{\rho} = \frac{\boldsymbol{r}_1 - \boldsymbol{r}_2}{\sqrt{2}}\,, \quad \boldsymbol{\lambda} = \frac{\boldsymbol{r}_1 + \boldsymbol{r}_2 - 2\boldsymbol{r}_3}{\sqrt{6}}\,, \tag{4.1.35}$$

because in this way one can remove the center-of-mass motion (which would have led to spurious excitations) to arrive at

$$H = \frac{\boldsymbol{p}_\rho^2}{2m} + \frac{\boldsymbol{p}_\lambda^2}{2m} + \sum_{i<j} V(\boldsymbol{r}_{ij})\,. \tag{4.1.36}$$

We could start with a harmonic oscillator potential $V(\boldsymbol{r}_{ij}) = k\boldsymbol{r}_{ij}^2/2$, which because of $\sum_{i<j} \boldsymbol{r}_{ij}^2 = 3\,(\boldsymbol{\lambda}^2 + \boldsymbol{\rho}^2)$ leads to two independent spherical harmonic oscillators

$$H = \left(\frac{\boldsymbol{p}_\rho^2}{2m} + \frac{3k}{2}\,\boldsymbol{\rho}^2\right) + \left(\frac{\boldsymbol{p}_\lambda^2}{2m} + \frac{3k}{2}\,\boldsymbol{\lambda}^2\right) \tag{4.1.37}$$

with frequency $\omega_0 = \sqrt{3k/m}$. The resulting baryon spectrum is then $E_N = E_0 + N\omega_0$, where E_0 is the ground-state energy, $N = 2n + l$, $n = n_\rho + n_\lambda$ and $l = l_\rho + l_\lambda$, and n_α and l_α are the radial and orbital excitations of the oscillators. The total angular momentum $\boldsymbol{J} = \boldsymbol{L} + \boldsymbol{S}$ is the sum of the total quark spin $\boldsymbol{S} = \sum_i \boldsymbol{s}_i$ and the orbital angular momentum $\boldsymbol{L} = \boldsymbol{l}_\rho + \boldsymbol{l}_\lambda$, which takes the values $L = |l_\rho - l_\lambda| \ldots l_\rho + l_\lambda$. The parity of a given state is $P = (-1)^l$. For example, the ground state is given by

$$\phi_{\text{grd}} = \left(\frac{m\omega_0}{\pi}\right)^{\frac{3}{2}} \exp\left[-\frac{m\omega_0}{2}\,(\boldsymbol{\rho}^2 + \boldsymbol{\lambda}^2)\right]. \tag{4.1.38}$$

Combined with $SU(6)$ for spin and flavor, where the quarks are assigned to the fundamental **6** representation ($u\uparrow$, $d\uparrow$, $s\uparrow$, $u\downarrow$, $d\downarrow$, $s\downarrow$), the harmonic oscillator potential results in the band structure discussed earlier around Table 3.5.

A pure oscillator spectrum with $E_N \propto N$ does not describe the baryon spectrum particularly well, since all states in Table 3.5 with the same N would be mass-degenerate. However, it provides a useful calculational basis for further refinements. For example, one can solve the Schrödinger equation in terms of the oscillator potentials and evaluate anharmonic parts of the potential perturbatively in the oscillator basis.

The prototype of a nonrelativistic quark model is the one by **de Rujula, Georgi** and **Glashow** from 1975. It employs the Breit-Fermi interaction for one-gluon exchange, which breaks $SU(3)_f$ symmetry due to the different light and strange-quark masses and $SU(2)$ spin symmetry due to its spin-dependent interactions. For ground states the important part is the spin-spin contact interaction, which leads to mass formulas of the form

$$M = \sum_i m_i + \frac{2\alpha_s}{3}\,\frac{8\pi}{3}\left\langle \delta^3(\boldsymbol{r}) \sum_{i<j} \frac{\boldsymbol{s}_i \cdot \boldsymbol{s}_j}{m_i m_j} \right\rangle. \tag{4.1.39}$$

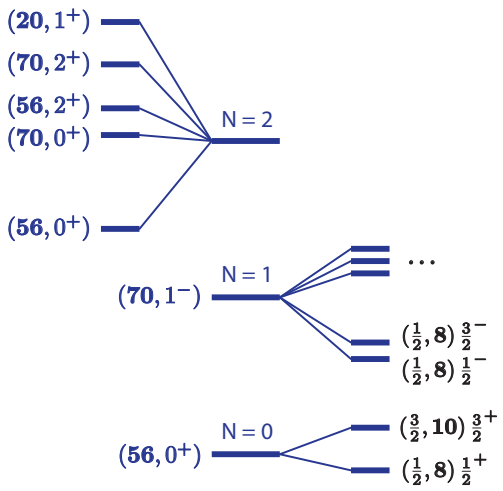

FIG. 4.2: Baryon mass splittings in the quark model (same notation as in Table 3.5).

In the limit of $SU(3)_f$ symmetry, the mass splitting from the spin-spin interactions can be determined like in Eq. (4.1.16) from $\boldsymbol{S} = \boldsymbol{s}_1 + \boldsymbol{s}_2 + \boldsymbol{s}_3$ and therefore

$$\sum_{i<j} \langle \boldsymbol{s}_1 \cdot \boldsymbol{s}_2 \rangle = \frac{S(S+1) - \frac{9}{4}}{2} = \pm \frac{3}{4} \,. \tag{4.1.40}$$

In this way, the ground-state octet baryons satisfy

$$\begin{aligned} M_N &= M_0 + 3m_n \,, \\ M_\Lambda = M_\Sigma &= M_0 + 2m_n + m_s \,, \\ M_\Xi &= M_0 + m_n + 2m_s \end{aligned} \tag{4.1.41}$$

where $m_{n,s}$ are the light and strange quark masses and the decuplet masses only differ by the spin splitting. This reproduces phenomenological **Gell-Mann-Okubo relations** such as $M_{\Sigma^*} - M_\Sigma = M_{\Xi^*} - M_\Xi$, whereas for $m_s \neq m_n$ they pick up corrections.

Another influential quark model has been the **Isgur-Karl model**, which implements a harmonic oscillator potential together with an anharmonic perturbation, a confinement part and a hyperfine interaction. The spin-orbit interactions are neglected since their inclusion would spoil the agreement with the spectrum (the resulting mass splittings tend to be too large). This leads to the pattern in Fig. 4.2, where the splitting between the $N = 0$ states is due to the spin-spin contact term, the splittings in the $N = 1$ band come from the spin-spin contact and tensor terms, and the splittings between the $SU(6)$ multiplets in the $N = 2$ band are due to the anharmonic perturbation. The Isgur-Karl model provides a good description of the light and strange baryon spectrum but also predicts more states than observed; however, it also predicts that most of those unobserved states are weakly coupled to the πN channel.

Many quark potential models have been constructed following up on the early developments, including relativized models, flux-tube and instanton-induced models, Goldstone-boson exchange models, diquark-based models and more.[1]

[1] For a review, see Capstick and Roberts, Prog. Part. Nucl. Phys. 45 (2000) 241, nucl-th/0008028.